Inorg. Chem. **2002**, *41*, 3032–3041

New N_3S Donor Ligand Small Peptide Analogues of the *N*-Mercaptoacetyl-glycylglycylglycine Ligand in the Clinically Used Tc-99m Renal Imaging Agent: Evidence for Unusual Amide Oxygen Coordination by Two New Ligands

Malgorzata Lipowska,[†] Lory Hansen,[†] Xiaolong Xu,[†] Patricia A. Marzilli,[‡] Andrew Taylor, Jr.,[†] and Luigi G. Marzilli*,[‡]

Departments of Radiology and Chemistry, Emory University, Atlanta, Georgia 30322

Received December 28, 2001

Three new X-ray structurally characterized Re(V)O complexes, $ReO(MEG_3H_2)$ (**10**), $ReClO(MAEG_2H_3)$ (**11**), and $\{ReO(MECG_2H_2)\}_2$ (**12**), were prepared from protected forms of three new ligands, mercaptoethyl-glycylglycylglycine (MEG_3H_5), mercaptoacetamide-ethyl-glycylglycine ($MAEG_2H_5$), and mercaptoethyl-carbamoylmethyl-glycylglycine ($MECG_2H_5$). (Subscript on H indicates the number of dissociable protons.) Mercaptoacetyltriglycine (MAG_3H_5) is the ligand precursor for the clinically used Tc-99m renal imaging agent. The new potentially N_3S donor ligands have a glycylglycine carboxyl end as in MAG_3H_5, but a secondary amine (sp^3 N) replaces one amide (sp^2 N) of MAG_3H_5. $ReO(MEG_3H_2)$ (**10**) is a typical five-coordinate pseudo-square-pyramidal complex with the oxo ligand at the apex and the trianionic form of MEG_3H_5 coordinated in the basal plane via N_3S. In the other complexes, the quadridentate ligand has N_2OS ligation, with the carbonyl oxygen of the glycyl amide group coordinated trans to the oxo ligand. This unusual ligation mode, which is facilitated by the preferred endo configuration of the ligated glycyl sp^3 N, leaves a vacant basal coordination site. In **11**, the chloro ligand completes the equatorial plane, whereas, in **12**, a glycine carboxylate oxygen of the ligand on the partner Re completes the equatorial plane. Both complexes thus possess an unexpected pseudo-octahedral geometry. For **10**, **11**, and **12**, the ^1H NMR spectra, monitored from high to low pH, exhibited changes only when the pH was lowered below 6. This finding indicates that at physiological pH these complexes possess the desirable characteristic of existing as one monomeric species having only one ionization state, with the coordinated sp^3 N deprotonated. Below pH 6 and above pH $\sim$4, changes in the ^1H NMR shifts indicate that this sp^3 N has become protonated. Thus, the N_3S ligands in all three complexes exhibit normal coordination above pH $\sim$4. However, X-ray data for **11** and **12** and some NMR evidence for **11** indicate that the ligands of the two complexes rearrange at low pH (<3). The striking differences between the solution- and solid-state structures reinforce the caveat that solution structural studies conducted at physiological pH are necessary in order to gain insight into the nature of radiopharmaceuticals.

Introduction

Because the structure, overall charge, and charge distribution of $^{99m}Tc(V)O$ radiopharmaceuticals influence their biodistribution, our goal is to improve upon current knowledge of Tc and Re coordination chemistry; such knowledge should allow us to develop radiopharmaceuticals in a more rational manner than is possible today. In particular, we are seeking new ligands allowing the preparation of $^{99m}Tc(V)O$ agents that are rapidly cleared by the kidneys, that can be produced in solution in a single isomeric form, and that exist in one ionization state at physiological pH. The two renal agents used clinically are the $^{99m}Tc(V)O$ complexes formed from mercaptoacetyltriglycine (MAG_3H_5, Chart 1)[1−5] and

* To whom correspondence should be addressed. E-mail: lmarzil@emory.edu.
[†] Department of Radiology.
[‡] Department of Chemistry.

(1) Fritzberg, A. R.; Kasina, S.; Eshima, D.; Johnson, D. L. *J. Nucl. Med.* **1986**, *27*, 111−116.
(2) Taylor, A.; Eshima, D.; Christian, P. E.; Milton, W. *Radiology* **1987**, *162*, 365−370.
(3) Taylor, A.; Eshima, D.; Alazraki, N. *Eur. J. Nucl. Med.* **1987**, *12*, 510−514.

10.1021/ic011325z CCC: $22.00
Published on Web 05/10/2002

Chart 1

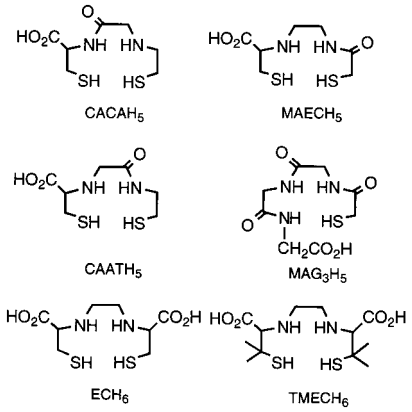

from *N*,*N*′-ethylene-di-L-cysteine (LL-ECH_6, Chart 1).[6−8] (Subscript on H indicates the number of dissociable protons.) The complexes formed from MAG_3H_5 and ECH_6 differ in that all N donors in the former are sp^2 amido donors lacking a dissociable NH group, whereas the latter have two secondary amines which can coordinate either as the sp^3 NH group or as an sp^3 N lacking an attached proton. Both classes of agents have dangling carboxyl groups, a feature associated with high renal clearance. However, these agents, although used clinically, do not have optimal renal clearance.[8−12] Two strategies to design better agents can be based on these agents: first, make ECH_6 derivatives that are more like MAG_3H_5; and second, make MAG_3H_5 derivatives that are more like ECH_6. Adopting the first strategy, we previously found agents with excellent renal imaging properties.[13,14] This report describes studies that utilize the second strategy. In the Discussion section, we compare the advantages and limitations of the two strategies, particularly with regard to stereochemistry.

In our preparations of ligands designed to have dangling carboxyl groups when coordinated, we often employ esters as starting materials and synthetic intermediates because compounds with carboxylic acid groups can be difficult to purify and have limited solubility in the organic solvents used for most ligand syntheses. We report here studies of Re

Scheme 1

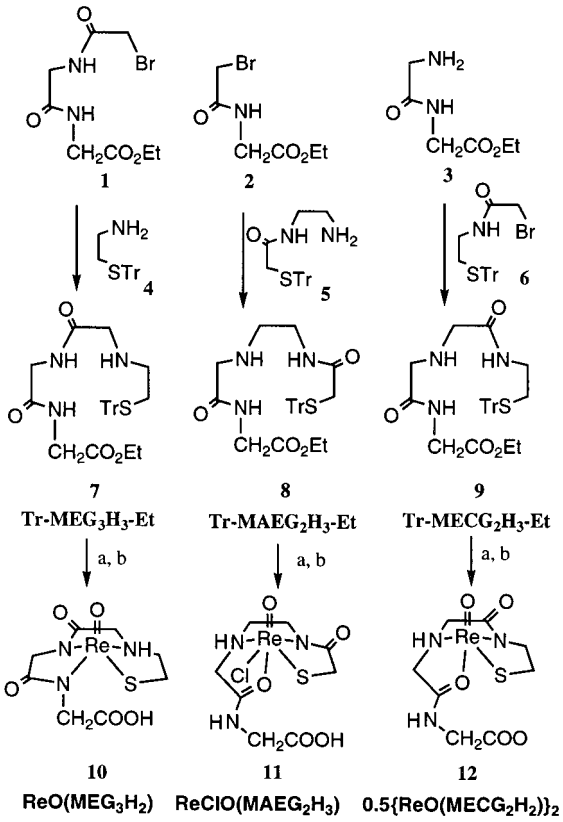

complexes prepared from three new protected amine−diamide−thiol N_3S ligands, Tr-MEG_3H_3-Et (**7**), Tr-$MAEG_2H_3$-Et (**8**), and Tr-$MECG_2H_3$-Et (**9**) (Tr = trityl, Scheme 1). We study the environmentally preferred Re analogues of ^{99m}Tc agents rather than the ^{99}Tc analogues because our experience shows with our classes of compounds that the Re chemistry serves as a useful guide in understanding the ^{99m}Tc imaging agents.

Traditionally, investigators have relied on single-crystal X-ray characterization of ^{99}Tc or Re radiopharmaceutical analogues, but often, the solid-state form does not correspond to the form of the complex in aqueous solution at physiological pH.[15] Special efforts must be made to isolate appropriate forms. For example, we characterized the dianionic form of $[ReO(MAG_3)]^{2-}$.[16] This is the protonation state expected for physiological pH, whereas a previous X-ray structural study examined the protonated monoanionic form.[17] However, it is often not possible to isolate or crystallize products from solutions under physiological conditions, especially for renal agents with dangling carboxyl groups. Therefore, much of our effort has been aimed at developing strategies that allow us to elucidate many features of the solution chemistry of radiopharmaceuticals at physiological pH.[15,18,19] In this report, we present evidence for

(4) Taylor, A.; Ziffer, J. A.; Eshima, D. *Eur. J. Nucl. Med.* **1990**, *15*, 371−378.
(5) Eshima, D.; Taylor, A. *Semin. Nucl. Med.* **1992**, *22*, 61−73.
(6) Jamar, F.; Stoffel, M.; Van Nerom, C.; Verbruggen, A.; Mourad, M.; Squifflet, J. P.; Beckers, C. *J. Nucl. Med.* **1993**, *34*, 129P.
(7) Van Nerom, C. G.; Claeys, C. W.; Mormans, G. M.; De Roo, M. J.; Verbruggen, A. M. In *Radionuclides in Nephrology*; O'Reilly, P. H., Taylor, A., Nally, J. V., Eds.; Field and Wood, Inc.: Blue Bell, PA, 1994; pp 13−20.
(8) Taylor, A.; Hansen, L.; Eshima, D.; Malveaux, E.; Folks, R.; Shattuck, L.; Lipowska, M.; Marzilli, L. G. *J. Nucl. Med.* **1997**, *38*, 821−826.
(9) Volkmann, R.; Friberg, P.; Jakobsson, L.; Jensen, G.; Jonsson, B.-A.; Moonen, M. In *Radionuclides in Nephrology*; O'Reilly, P. H., Taylor, A., Nally, J. V., Eds.; Field and Wood, Inc.: Blue Bell, PA, 1994; pp 21−26.
(10) Piepsz, A.; Tondenr, M.; Kinthaert, J.; Ham, H. R. *Eur. J. Nucl. Med.* **1996**, *23*, 195−198.
(11) Kotzerke, J.; Moog, F.; Kleinschmidt, K.; Reske, S. N. *Eur. J. Nucl. Med.* **1996**, *23*, 1074.
(12) Taylor, A.; Myrick, S.; Grant, S. *J. Nucl. Med.* **1999**, *40*, 52P.
(13) Hansen, L.; Lipowska, M.; Xu, X.; Taylor, A.; Marzilli, L. G. *Q. J. Nucl. Med.* **1998**, *42*, 33 (abstract).
(14) Hansen, L.; Lipowska, M.; Marzilli, L. G.; Taylor, A., Jr. *J. Nucl. Med.* **1996**, *37*, 17P (abstract).
(15) Marzilli, L. G.; Banaszczyk, M. G.; Hansen, L.; Kuklenyik, Z.; Cini, R.; Taylor, A., Jr. *Inorg. Chem.* **1994**, *33*, 4850−4860.
(16) Hansen, L.; Taylor, A., Jr.; Marzilli, L. G. *Met.-Based Drugs* **1995**, *2*, 105−110.
(17) Rao, T. N.; Adhikesavalu, D.; Camerman, A.; Fritzberg, A. R. *Inorg. Chim. Acta* **1991**, *180*, 63−67.
(18) Hansen, L.; Xu, X.; Yue, K. T.; Kuklenyik, Z.; Taylor, A.; Marzilli, L. G. *Inorg. Chem.* **1996**, *35*, 1958−1966.

isolated forms that are dramatically different from the forms present under physiological conditions. These new forms have unusual and interesting structures.

Experimental Section

Compounds **1** and **2** (see Scheme 1) were synthesized as described in the following paragraphs. Glycine ethyl ester hydrochloride and glycylglycine ethyl ester hydrochloride (**3**) were purchased from Sigma and used as received. *S*-Trityl-2-aminoethanethiol[20] (**4**), *N*-(2-aminoethyl)-2-(*S*-tritylmercapto)acetamide[21] (**5**), *N*-(2-bromoacetyl)-*S*-trityl-2-aminoethanethiol[20] (**6**), and $ReIO_2(PPh_3)_2$[22] were prepared by published methods. Column chromatography was conducted on Merck silica gel 60 (230−400 mesh ASTM). Elemental analyses were performed by Atlantic Microlabs, Atlanta, GA. ^{1}H NMR spectra were recorded on Varian 300 or 400 MHz spectrometers and referenced to internal tetramethylsilane (for $CDCl_3$ and DMSO-d_6) or sodium 3-(trimethylsilyl)propionate-d_4 (for D_2O).

Syntheses. *N*-(2-Bromoacetyl)glycylglycine Ethyl Ester (1). To a stirred −70 °C solution of glycylglycine ethyl ester hydrochloride (3.94 g, 20 mmol) and triethylamine (6.06 g, 60 mmol) in dry CH_2Cl_2 (50 mL) was added dropwise a solution of bromoacetyl bromide (4.04 g, 20 mmol) in CH_2Cl_2 (20 mL). The reaction mixture was allowed to warm to room temperature and then was quenched by adding water (50 mL). The layers were separated, and the organic portion was washed with 1 N HCl, water, and brine (50 mL each). The organic solution was dried over sodium sulfate, filtered, and concentrated. Flash chromatography (silica, $CHCl_3$), followed by crystallization from EtOH, provided a white solid. Yield, 66% (3.7 g). Anal. Calcd for $C_8H_{13}BrN_2O_4$: C, 34.18; H, 4.66; N, 9.97. Found: C, 34.43; H, 4.63; N, 9.98. ^{1}H NMR ($CDCl_3$): 1.27 (t, J = 7.2 Hz, 2H), 3.92 (s, 2H), 4.04 (d, J = 5.6 Hz, 2H), 4.07 (d, J = 5.6 Hz, 2H), 4.24 (q, J = 7.2 Hz, 2H), 6.55 (bs, 1H), 7.22 (bs, 1H).

***N*-(2-Bromoacetyl)glycine Ethyl Ester (2).** Compound **2** was prepared in a similar manner as **1** from glycine ethyl ester hydrochloride (4.17 g, 30 mmol) in 68% yield (4.58 g) after crystallization from EtOH. Anal. Calcd for $C_6H_{10}BrNO_3$: C, 32.16; H, 4.50; N, 6.25. Found: C, 32.34; H, 4.39; N, 6.08. ^{1}H NMR ($CDCl_3$): 1.31 (t, J = 7.2 Hz, 3H), 3.92 (s, 2H), 4.07 (d, J = 5.2 Hz, 2H), 4.25 (q, J = 7.2 Hz, 2H), 6.98 (bs, 1H).

***N*-[(*S*-Tritylmercapto)ethyl]glycylglycylglycine Ethyl Ester [Tr-MEG$_3$H$_3$-Et] (7).** A solution of *N*-(2-bromoacetyl)glycylglycine ethyl ester (**1**) (0.7 g, 2.5 mmol), *S*-trityl-2-aminoethanethiol (**4**) (0.8 g, 2.5 mmol), and sodium carbonate (0.53 g, 5 mmol) in anhydrous DMF (15 mL) was stirred overnight at room temperature. Chloroform (50 mL) was added, and the reaction mixture was filtered and concentrated. The resulting residue was purified by column chromatography (silica, 1%−10% EtOH/$CHCl_3$). The fraction containing the product was collected and reduced to dryness by rotary evaporation, leaving a pure foam. Yield, 57% (0.84 g). Anal. Calcd for $C_{29}H_{33}N_3O_4S\cdot HCl$: C, 62.63; H, 6.16; N, 7.55; S, 5.76; Cl, 6.38. Found: C, 62.62, H, 6.05; N, 7.39, S, 5.71; Cl, 6.68. ^{1}H NMR ($CDCl_3$): 1.27 (t, J = 7.2 Hz, 3H), 1.54 (bs, 1H), 2.37 (t, J = 6.0 Hz, 2H), 2.49 (t, J = 6.0 Hz, 2H), 3.14 (s, 2H), 3.95 (d, J = 6.0 Hz, 2H), 3.97 (d, J = 5.4 Hz, 2H), 4.19 (q, J = 7.2 Hz, 2H), 6.72 (t, J = 5.6 Hz, 1H), 7.19−7.30 (m, 9H), 7.39−7.42 (m, 6H), 7.79 (t, J = 5.6 Hz, 1H).

***N*-[[(*S*-Tritylmercapto)acetamide]ethyl]glycylglycine Ethyl Ester [Tr-MAEG$_2$H$_3$-Et] (8).** To the solution of *N*-(2-aminoethyl)-2-(*S*-tritylmercapto)acetamide (**5**) (1.65 g, 4 mmol) and triethylamine (1.2 g, 12 mmol) in anhydrous CH_2Cl_2 (20 mL) was added *N*-(2-bromoacetyl)glycine ethyl ester (**2**) (0.9 g, 4 mmol). The reaction mixture was stirred overnight at room temperature and then concentrated by rotary evaporation. The residue was purified by column chromatography (silica, 1−5% EtOH/$CHCl_3$). Fractions containing the product were collected and concentrated to dryness by rotary evaporation, giving a pure foam (1.6 g, 77%). Anal. Calcd for $C_{29}H_{33}N_3O_4S\cdot HCl$: C, 62.63; H, 6.16; N, 7.55; S, 5.76, Cl, 6.37. Found: C, 62.61; H, 6.03; N, 7.48; S, 5.56; Cl, 6.24. ^{1}H NMR ($CDCl_3$): 1.26 (t, J = 7.2 Hz, 3H), 1.62 (bs, 1H), 2.63 (t, J = 6.0 Hz, 2H), 3.07 (q, J = 6.0 Hz, 2H), 3.14 (s, 2H), 3.26 (s, 2H), 3.97 (d, J = 5.6 Hz, 2H), 4.14 (q, J = 7.2 Hz, 2H), 6.28 (t, J = 5.2 Hz, 1H), 7.23−7.31 (m, 9H), 7.39−7.42 (m, 6H), 7.57 (t, J = 5.2 Hz, 1H).

***N*-[[(*S*-Tritylmercapto)ethyl]carbamoylmethyl]glycylglycine Ethyl Ester [Tr-MECG$_2$H$_3$-Et] (9).** Compound **9** was synthesized by the method used for **8** starting from glycylglycine ethyl ester hydrochloride (**3**) (0.196 g, 1 mmol) and *N*-(2-bromoacetyl)-*S*-trityl-2-aminoethanethiol (**6**) (0.44 g, 1 mmol) in 40% yield (1.02 g). Anal. Calcd for $C_{29}H_{33}N_3O_4S\cdot HCl$: C, 62.63; H, 6.16; N, 7.55; S, 5.76, Cl, 6.37. Found: C, 62.65; H, 6.09; N, 7.34; S, 5.62; Cl, 6.59. ^{1}H NMR ($CDCl_3$): 1.28 (t, J = 7.2 Hz, 3H), 1.79 (bs, 1H), 2.44 (t, J = 6.4 Hz, 2H), 3.10 (q, J = 6.4 Hz, 2H), 3.23 (s, 2H), 3.31 (s, 2H), 3.98 (d, J = 5.6 Hz, 2H), 4.19 (q, J = 7.2 Hz, 2H), 6.56 (t, J = 5.6 Hz, 1H), 7.06 (t, J = 5.2 Hz, 1H), 7.20−7.30 (m, 9H), 7.39−7.41 (m, 6H).

General Procedure for Complexes. Triethylsilane (1.4 mmol) was added slowly to a solution of ligand **7**, **8**, or **9** (1.4 mmol) in trifluoroacetic acid (5 mL). The reaction mixture was partitioned between hexane (10 mL) and water (10 mL). The aqueous layer was separated, washed with hexane, filtered through Celite, and concentrated to dryness by rotary evaporation. The crude deprotected ligand was dissolved in 50% MeOH/H_2O (20 mL), and the pH was adjusted to 11 with 2 N NaOH. Solid purple $ReIO_2(PPh_3)_2$ (1.4 mmol) was added to the solution to give a suspension, and the reaction mixture was heated at reflux. The pH was maintained at 11 by dropwise addition of 2 N NaOH, during the first few hours, after which the pH remained at 11. After 10 h, the purple suspension had become an orange-brown solution. Cooled to room temperature, the solution was extracted with $CHCl_3$ and filtered through Celite. The aqueous filtrate was concentrated to ∼5 mL by rotary evaporation, acidified to pH 5 with 1 N HCl, and passed down a column of Sephadex G-15 (eluting with deionized water). The orange fraction containing the complex was collected and reduced in volume by rotary evaporation. The pH of the solution was adjusted to ∼3 with 1 N HCl (a change in solution color was observed for **11** (purple) and **12** (pink-violet); the solution of **10** remained orange). The crystalline solid formed by slow evaporation was collected, washed with water, and vacuum-dried.

ReO(MEG$_3$H$_2$) (10). Orange-brown crystals in 35% yield. Anal. Calcd for $C_8H_{12}N_3O_5ReS\cdot 3/4H_2O$: C, 20.79; H, 2.95; N, 9.09; S, 6.94. Found: C, 20.72; H, 2.95; N, 9.06; S, 6.93.

ReClO(MAEG$_2$H$_3$) (11). Purple crystals in 26% yield. Anal. Calcd for $C_8H_{13}ClN_3O_5ReS\cdot H_2O$: C, 19.11; H, 3.01; N, 8.35; S, 6.37, Cl, 7.04. Found: C, 19.28; H, 3.03; N, 8.27; S, 6.31; Cl, 6.98.

{ReO(MECG$_2$H$_2$)}$_2$ (12). Violet crystals in 19% yield. Anal. Calcd for $C_{16}H_{24}N_6O_{10}Re_2S_2\cdot 2H_2O$: C, 20.60; H, 3.02; N, 9.01; S, 6.87. Found: C, 20.76; H, 2.83; N, 8.86; S, 6.81.

(19) Hansen, L.; Yue, K. T.; Xu, X.; Lipowska, M.; Taylor, A.; Marzilli, L. G. *J. Am. Chem. Soc.* **1997**, *119*, 8965−8972.
(20) O'Neil, J. P.; Wilson, S. R.; Katzenellenbogen, J. A. *Inorg. Chem.* **1994**, *33*, 319−323.
(21) Atkinson, E. R.; Handrick, G. R.; Bruni, R. J.; Granchelli, F. E. *J. Med. Chem.* **1965**, *8*, 29−33.
(22) Ciani, G. F.; D'Alfonso, G.; Romiti, P.; Sironi, A.; Freni, M. *Inorg. Chim. Acta* **1983**, *72*, 29−37.

X-ray Crystallography. The syntheses of complexes **10**−**12** described in a previous paragraph afforded well-shaped crystals suitable for X-ray diffraction study, with no need to recrystallize. Crystals of $ReO(MEG_3H_2)\cdot H_2O$ (**10**) (0.30 × 0.32 × 0.38 mm^3), $ReClO(MAEG_2H_3)\cdot H_2O$ (**11**) (0.28 × 0.28 × 0.32 mm^3), and $\{ReO(MECG_2H_2)\}_2\cdot 2H_2O$ (**12**) (0.27 × 0.12 × 0.04 mm^3) were used for data collection. Compounds **10** and **11** were mounted under Paratone-8277 on a glass fiber and immediately placed in a cold nitrogen stream at 193 K on a standard Siemens SMART CCD Area Detector System equipped with a normal focus Mo-target X-ray tube. Data were collected by using a narrow frame method with scan widths of 0.3° in ω and exposure times of 30 s/frame. Frames were integrated to a maximum 2θ angle of 56.7° for **10** and 56.6° for **11** with the Siemens SAINT program. Data were corrected for absorption.[23] A suitable crystal of **12** was coated with Paratone N oil, suspended in a small fiber loop, and placed in a cooled nitrogen gas stream at 100 K on a Bruker D8 SMART APEX CCD sealed tube diffractometer with graphite monochromated Mo Kα (0.71073 Å) radiation. Data were measured using a series of combinations of φ and ω scans with 10 s frame exposures and 0.3° frame widths. Data collection, indexing, and initial cell refinements were all carried out using SMART[24] software. Frame integration and final cell refinements were done using SAINT[25] software. The final cell parameters were determined from least-squares refinement on 9715 reflections. Absorption corrections were made with the SADABS[26] program.

The structures of **10**, **11**, and **12** were determined by direct methods and difference Fourier techniques and refined on F^2 (SHELXL 93[27] for **10** and **11**, and SHELXTL, V5.10[28] for **12**). All non-hydrogen atoms were refined anisotropically. The water, amine, and carboxyl H atoms were located from a late-stage difference map and their positions refined. H atoms bound to carbon were generated at calculated positions (d(C−H) = 0.96 Å). All H atoms were constrained by using a riding model with isotropic thermal parameters that were 20% greater than the U(eq) of the heavy bonded atom. Table 1 lists crystal data and refinement parameters for **10**, **11**, and **12**.

Table 1. Crystal Data and Structure Refinement for $ReO(MEG_3H_2)\cdot H_2O$ (**10**), $ReClO(MAEG_2H_3)\cdot H_2O$ (**11**), and $\{ReO(MECG_2H_2)\}_2\cdot 2H_2O$ (**12**)

	10	**11**	**12**
empirical formula	$C_8H_{14}N_3O_6ReS$	$C_8H_{15}ClN_3O_6ReS$	$C_{16}H_{28}N_6O_{12}Re_2S_2$
fw	466.48	502.94	932.96
T (K)	193(2)	193(2)	100(2)
λ (Å)	0.71073	0.71073	0.71073
space group	$P2_1/n$	$P2_1/c$	$P2_1/n$
unit cell dimensions			
a (Å)	8.358(2)	7.771(2)	8.798(17)
b (Å)	12.356(2)	11.105(2)	10.526(2)
c (Å)	12.650(3)	16.575(3)	13.427(3)
β (deg)	106.13(3)	101.23(3)	95.24(4)
V (Å^3)	1255.0(5)	1403.0(5)	1238.2(4)
Z	4	4	2
ρ_{calc} (mg/m^3)	2.469	2.381	2.502
abs coeff (mm^{-1})	9.877	9.028	10.010
R indices	R1 = 0.0233	R1 = 0.0179	R1 = 0.0463
[$I > 4\sigma(I)$]	wR2 = 0.0583	wR2 = 0.0445	wR2 = 0.1076
R indices	R1 = 0.0264	R1 = 0.0194	R1 = 0.0564
(all data)[a]	wR2 = 0.0593	wR2 = 0.0450	wR2 = 0.1108

[a] $R1 = (\sum||F_o| - |F_c||)/\sum|F_o|$; $wR2 = [\sum[w(F_o^2 - F_c^2)^2]/\sum[w(F_o^2)^2]]^{1/2}$ where $w = 1/[\sigma^2(F_o^2) + (aP)^2 + bP]$ and $P = [(\mathrm{Max};0,F_o^2) + 2F_c^2]/3$.

Chart 2

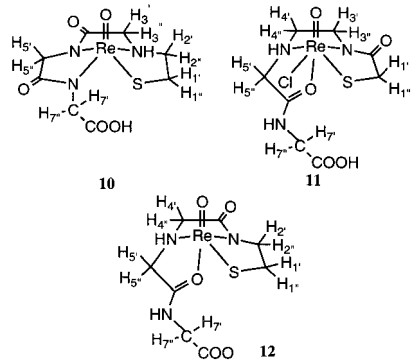

Results

Synthesis. Scheme 1 illustrates the synthetic routes utilized in the preparation of the amine−diamide−thiol N_3S ligands, Tr-MEG_3H_3-Et (**7**), Tr-$MAEG_2H_3$-Et (**8**), and Tr-$MECG_2H_3$-Et (**9**). Precursors **1** and **2** were obtained by *N*-acylation of glycylglycine ethyl ester and glycine ethyl ester, respectively, with bromoacetyl bromide in CH_2Cl_2 in the presence of triethylamine. *N*-Alkylation of **4**,[20] **5**,[21] and **3** with **1**, **2**, and **6**,[20] respectively, afforded the respective *S*-trityl-protected ethyl esters in good yield (**7**, 57%; **8**, 77%; **9**, 40%). Ligands **7**−**9** were treated with Et_3SiH in TFA to remove the trityl-protected group. Hydrolysis of the ester group was achieved in situ under the basic conditions used to form the complexes from $ReIO_2(PPh_3)_2$. [The syntheses employed a ligand exchange reaction because we are trying to assess the likely ligand binding modes to Tc, not to simulate the preparations of Re radiopharmaceuticals. It is well known that for the same ligand direct reduction of MO_4^- affords M(V)O complexes more easily when M = ^{99m}Tc, ^{99}Tc than when M = Re (ReO_4^- is more difficult to reduce then TcO_4^-).[29−32]] After purification by gel filtration, the solutions were allowed to evaporate slowly to afford X-ray quality crystals of $ReO(MEG_3H_2)$ (**10**), $ReClO(MAEG_2H_3)$ (**11**), and $\{ReO(MECG_2H_2)\}_2$ (**12**). Analytical data obtained for these complexes are consistent with the formulations depicted in Chart 2 (only half the dinuclear complex **12** is shown). The color of an aqueous solution of **10** was insensitive to pH, remaining orange under both basic and acidic conditions. However, solutions of **11** and **12** changed in color from orange at neutral and basic pHs to purple or pink-violet, respectively, as the pH became acidic.

(23) Blessing, R. H. *Acta Crystallogr., Sect A* **1995**, *51*, 33−38.
(24) *SMART*, Version 5.624; Bruker AXS, Inc.: Madison, WI, 2000.
(25) *SAINT*, Version 6.02; Bruker AXS, Inc.: Madison, WI, 2000.
(26) Sheldrick, G. *SADABS*, Version 2.03; University of Göttingen: Göttingen, Germany, 2001.
(27) Sheldrick, G. *SHELX 93*; University of Göttingen: Göttingen, Germany, 1993.
(28) *SHELXTL*, Version 5.10; Bruker AXS, Inc.: Madison, WI, 2000.
(29) Francesconi, L. C.; Graczyk, G.; Wehrli, S.; Shaikh, S. N.; McClinton, D.; Liu, S.; Zubieta, J.; Kung, H. F. *Inorg. Chem.* **1993**, *32*, 3114−3124.
(30) Rao, T. N.; Adhikesavalu, D.; Camerman, A.; Fritzberg, A. R. *J. Am. Chem. Soc.* **1990**, *112*, 5798−5804.
(31) Grummon, G.; Rajagopalan, R.; Palenik, G. J.; Koziol, A. E.; Nosco, D. L. *Inorg. Chem.* **1995**, *34*, 1764−1772.
(32) Edwards, D. S.; Cheesman, E. H.; Watson, M. W.; Maheu, L. J.; Nguyen, S. A.; Dimitre, L.; Nason, T.; Watson, A. D.; Walovitch, R. In *Technetium and Rhenium in Chemistry and Nuclear Medicine 3*; Nicolini, M., Bandoli, G., Mazzi, U., Eds.; Cortina International: Verona, 1990; pp 433−444.

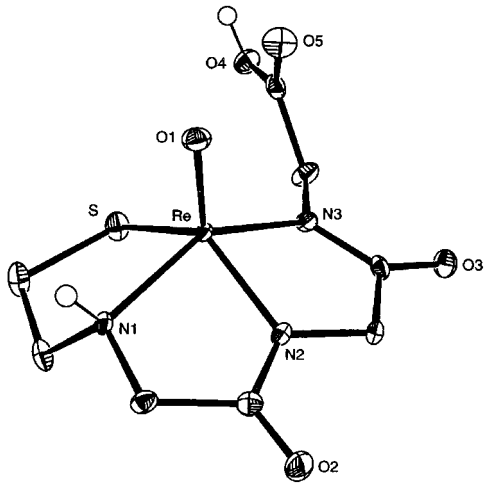

Figure 1. Perspective drawing of $ReO(MEG_3H_2)$ (**10**) with 50% probability for the thermal ellipsoids.

X-ray Crystallography. $ReO(MEG_3H_2)$ (**10**) is a five-coordinate pseudo-square-pyramidal complex, with the oxo ligand coordinated at the apex and the N_3S ligand coordinated in the basal plane (Figure 1). The terminal carboxyl group is syn to the oxo ligand. All Re−heteroatom bond distances are normal.[15,30,33−35] The Re atom is displaced from the basal plane (defined by N(1), N(2), N(3), and S) toward the oxo ligand (0.754 Å), and the O(1)−Re−N and O(1)−Re−S bond angles are >90° (Table 2); these features are typical of five-coordinate $ReO(N_2S_2)$ and $ReO(N_3S)$ complexes.[16,30,35,36]

$ReClO(MAEG_2H_3)$ (**11**) is a six-coordinate, pseudo-octahedral complex having two cis monodentate ligands (axial oxo ligand and equatorial chloro ligand), and the quadridentate ligand adopting N_2OS ligation (Figure 2). The thiol (S), amide N(1), and amine N(2) of the ligand occupy three equatorial coordination sites, and the amide O(3) is coordinated trans to the oxo ligand. The Re−N(1) (1.999(2) Å) and Re−N(2) (2.213(2) Å) distances are long. Re−N (amido) distances are normally significantly shorter than the Re−N (amine) distance. In **11**, the Re−N(1) (amido) distance (1.999(2) Å) is comparable to a typical Re−N (amine) bond distance (2.001(4)−2.154(13) Å), and the Re−N(2) (amine) distance (2.213(2) Å) is significantly longer than a typical R−N (amine) bond distance.[15,33,34] All other Re−heteroatom distances (Table 2), including the Re−Cl distance (2.406(9) Å), are normal.[37−39]

$\{ReO(MECG_2H_2)\}_2$ (**12**) is also a six-coordinate, pseudo-octahedral complex with the quadridentate ligand adopting N_2OS ligation and the amide O(3) coordinated trans to the oxo ligand (Figure 3). The molecule is actually a dinuclear species, with the glycine carboxylate O(4A) of the ligand on the partner Re completing the equatorial plane. The Re−O(4A) distance is 2.128(4) Å (Table 2). As expected, the weakness of the ligating ability of amide oxygen and the position trans to oxo group leads to longer Re−O(3) distances. These distances, 2.224(2) Å in **11** and 2.205(4) Å in **12**, are similar to M−O distances in related compounds in which the ligating oxygen is from a carboxyl group: *anti*-ReO(DL-ethylene-di-pen) (pen = penicillamine),[40] 2.200(8) Å; $^{99}TcO(D\text{-}penH_2)(D\text{-}penH_3)$,[41] 2.214(4) Å; and ReO(ethylene-di-L-cysteine),[15] 2.252(9) Å. Although the Re−O(3) interaction is weak, the Re atom moves closer to the basal plane in **11** and **12**, being displaced only 0.396 and 0.392 Å, respectively.

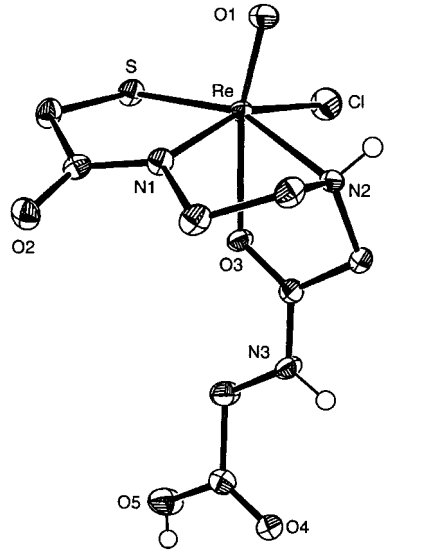

Figure 2. Perspective drawing of $ReClO(MAEG_2H_3)$ (**11**) with 50% probability for the thermal ellipsoids.

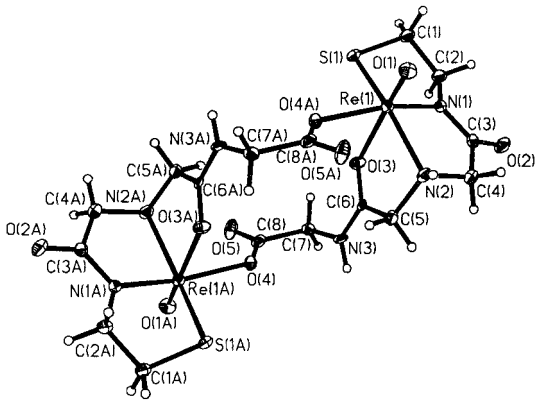

Figure 3. Perspective drawing of $\{ReO(MECG_2H_2)\}_2$ (**12**) with 50% probability for the thermal ellipsoids.

NMR Spectroscopy. ^1H NMR spectra of $ReO(MEG_3H_2)$ (**10**), $ReClO(MAEG_2H_3)$ (**11**), and $\{ReO(MECG_2H_2)\}_2$ (**12**) in aqueous solution were studied as a function of pH (Figures 4 to 7). At pH ∼11, the spectra contain sharp signals from

(33) Hansen, L.; Xu, X.; Lipowska, M.; Taylor, A., Jr.; Marzilli, L. G. *Inorg. Chem.* **1999**, *38*, 2890−2897.
(34) Hansen, L.; Lipowska, M.; Melendez, E.; Xu, X.; Hirota, S.; Taylor, A. T.; Marzilli, L. G. *Inorg. Chem.* **1999**, *38*, 5351−5358.
(35) Hansen, L.; Cini, R.; Taylor, A., Jr.; Marzilli, L. G. *Inorg. Chem.* **1992**, *31*, 2801−2808.
(36) Hansen, L.; Taylor, A., Jr.; Marzilli, L. G. *Met.-Based Drugs* **1994**, *1*, 31−39.
(37) Fortin, S.; Beauchamp, A. L. *Inorg. Chim. Acta* **1998**, *279*, 159−164.
(38) Hansen, L.; Alessio, E.; Iwamoto, M.; Marzilli, P. A.; Marzilli, L. G. *Inorg. Chim. Acta* **1995**, *240*, 413−417.
(39) Pearson, C.; Beauchamp, A. L. *Acta Crystallogr.* **1994**, *C50*, 42−44.
(40) Hansen, L.; Hirota, S.; Xu, X.; Taylor, A. T.; Marzilli, L. G. *Inorg. Chem.* **2000**, *39*, 5731−5740.
(41) Franklin, K. J.; Howard-Lock, H. E.; Lock, C. J. L. *Inorg. Chem.* **1982**, *21*, 1941−1946.

Table 2. Selected Bond Distances (Å) and Angles (deg) for $ReO(MEG_3H_2)\cdot H_2O$ (**10**), $ReClO(MAEG_2H_3)\cdot H_2O$ (**11**), and $\{ReO(MECG_2H_2)\}_2\cdot 2H_2O$ (**12**)

Bond Distances (Å)

10		**11**		**12**	
Re−O(1)	1.674(3)	Re−O(1)	1.677(2)	Re−O(1)	1.676(5)
Re−N(1)	2.116(3)	Re−N(1)	1.999(2)	Re−N(1)	1.988(5)
Re−N(2)	1.976(3)	Re−N(2)	2.213(2)	Re−N(2)	2.190(5)
Re−N(3)	2.019(3)	Re−O(3)	2.224(2)	Re−O(3)	2.205(4)
Re−S	2.2657(13)	Re−S	2.2808(8)	Re−S	2.2784(14)
		Re−Cl	2.4064(9)	Re−O(4A)	2.128(4)

Bond Angles (deg)

10		**11**		**12**	
O(1)−Re−N(1)	104.48(13)	O(1)−Re−N(1)	103.90(11)	O(1)−Re−N(1)	105.6(2)
O(1)−Re−N(2)	117.25(14)	O(1)−Re−N(2)	94.37(10)	O(1)−Re−N(2)	96.8(2)
O(1)−Re−N(3)	109.56(14)	N(1)−Re−N(2)	80.32(9)	N(1)−Re−N(2)	80.69(19)
N(2)−Re−N(3)	78.36(14)	O(1)−Re−O(3)	166.02(9)	O(1)−Re−O(3)	164.21(18)
N(2)−Re−N(1)	78.91(13)	N(1)−Re−O(3)	78.68(9)	N(1)−Re−O(3)	84.94(17)
N(3)−Re−N(1)	144.94(13)	N(2)−Re−O(3)	72.36(8)	N(2)−Re−O(3)	72.99(17)
O(1)−Re−S	113.23(11)	O(1)−Re−S	106.04(8)	O(1)−Re−S	105.91(16)
N(1)−Re−S	83.95(9)	N(1)−Re−S	84.89(7)	N(1)−Re−S	83.79(14)
N(2)−Re−S	129.23(10)	N(2)−Re−S	157.19(6)	N(2)−Re−S	155.29(14)
N(3)−Re−S	90.15(10)	O(3)−Re−S	87.82(6)	O(3)−Re−S	86.62(11)
		O(1)−Re−Cl	97.18(8)	O(1)−Re−O(4A)	94.97(18)
		N(1)−Re−Cl	158.67(7)	N(1)−Re−O(4A)	159.40(18)
		N(2)−Re−Cl	95.09(7)	N(2)−Re−O(4A)	98.28(17)
		O(3)−Re−Cl	80.09(6)	O(3)−Re−O(4A)	74.19(15)
		S−Re−Cl	92.41(3)	S−Re−O(4A)	89.58(11)

the ethylene bridge (four multiplets), the two acetyl residues (four strongly coupled doublets, each with $J \sim 18$ Hz), and the terminal glycine methylene group (two strongly coupled doublets, $J \sim 17$ Hz). Chart 2 shows the labeling of the hydrogens. Assignments of the CH signals for the ethylene bridge and the acetyl group closest to the thiolate end of each ligand were made through the obvious similarity to the respective previously assigned spectra of compounds with similar residues (e.g., **10** with *syn*-$ReO(CACAH_2)$,[33] **11** with *syn*-$ReO(MAECH_2)$,[34] and **12** with *syn*-$ReO(CAATH_2)$[42] (cf. Chart 1 for ligand definitions)). Signals for the protons of the terminal glycine (H_7'/H_7''; two doublets) had generally similar chemical shifts for all three complexes (Table 3). The two remaining strongly coupled doublets ($J \sim 18$ Hz) were assigned to the N-terminal acetyl group.

The ^{1}H NMR spectra of **10**−**12** in D_2O were monitored as the pH was lowered (Table 3). For **12**, no spectral changes were observed from pH 11 to 4.6 (Figure 7). Below pH 4, all signals remained sharp, and only small shift changes were observed for the H_2'/H_2'', H_1'' and the H_7'/H_7'' signals. The complex began to precipitate below pH 3.

For **10** and **11** (Figures 4−6), no NMR spectral changes were observed from pH 11 to ∼6. Below pH 6, the signals shifted, and broadening was observed for the H_1'/H_1'' and H_2'/H_2'' signals for **10** in the pH range 6−4 (Figure 4). Below pH 4, the signals sharpened again. The broadening of the signals near the NH pK_a (∼5) is due to NH/N$^-$ exchange and is consistent with the coexistence of monoanion and dianion forms exchanging at an intermediate rate on the NMR time scale.[15,40] Signals did not broaden for **11** (Figure 5) as was found for **10**. In contrast to the near absence of shifting for **12**, large signal shifts were observed for H_2'/H_2'' and H_3'/H_3'' signals for **10** (Figure 4) and H_4'/H_4'' and H_5'/H_5'' signals for **11** (Figure 5), respectively, in the pH range 6−4. Because these signals are from methylene groups bound directly to an sp^3 amine nitrogen atom, the shift patterns are consistent with protonation of this coordinated N at lower pH (pK_a ∼4.5 for NH of **11**).

Table 3. ^{1}H NMR (D_2O) Chemical Shifts (ppm) and Assignments for $ReO(MEG_3H_2)$ (**10**), $ReClO(MAEG_2H_3)$ (**11**), and $ReO(MECG_2H_2)$ (**12**) in Neutral and Anionic Forms

	C_1		C_2		C_3		C_4		C_5		C_7	
pH	$H_{1'}$	$H_{1''}$	$H_{2'}$	$H_{2''}$	$H_{3'}$	$H_{3''}$	$H_{4'}$	$H_{4''}$	$H_{5'}$	$H_{5''}$	$H_{7'}$	$H_{7''}$
						10						
9.6	2.69	3.28	4.03	3.09	5.02	4.30			4.43	4.34	4.93	4.55
5.6	2.72	3.29	3.96	2.94	4.97	4.27			4.38	4.38	4.99	4.58
4.3	2.96	3.32	3.72	2.42	*a*	4.16			4.43	4.27	5.20	4.67
3.1	3.06	3.34	3.63	2.26	*a*	4.12			4.46	4.24	5.31	*a*
						11						
11.7	3.96	4.32			3.52	4.57	3.26	4.08	4.87	3.92	4.99	4.59
5.8	3.96	4.35			3.53	4.56	3.22	4.06	*a*	3.91	5.00	4.61
4.8	3.97	4.47			3.55	4.56	3.03	3.96	4.76	3.86	5.05	4.68
3.8	3.99	4.65			3.58	4.55	2.75	3.88	4.64	3.79	5.12	*a*
2.1	4.01	*a*			3.61	4.55	2.48	3.80	4.56	3.80	5.18	4.95
						12						
11.0	3.09	2.91	3.27	4.43			4.77	4.20	5.00	3.87	5.11	4.59
4.5	3.09	2.91	3.28	4.42			4.75	4.19	4.99	3.86	5.17	4.66
3.6	3.10	2.96	3.33	4.40			4.74	4.18	4.98	3.95	5.24	4.75

[a] Signal overlaps with water peak.

Below pH 4, the H_2'' signal of **10** and the H_4' signal of **11** shifted appreciably. The H_1' signal of **10** and the H_1'' signal of **11**, as well as the H_7'/H_7'' signals for both **10** and **11**, also shifted significantly. The shifting of the H_7'/H_7'' signals for all three complexes was largest below pH 4, consistent with protonation of the ionized carboxylate group. At low pH (∼3), new ^{1}H NMR signals for **11** (Figure 6) emerged, suggesting a rearrangement of the ligand consistent with the unusual N_2OS ligation observed in the X-ray structure.

(42) Lipowska, M.; Hansen, L.; Cini, R.; Choi, H.; Xu, X.; Taylor, A. T.; Marzilli, L. G. *Inorg. Chim. Acta*, in press.

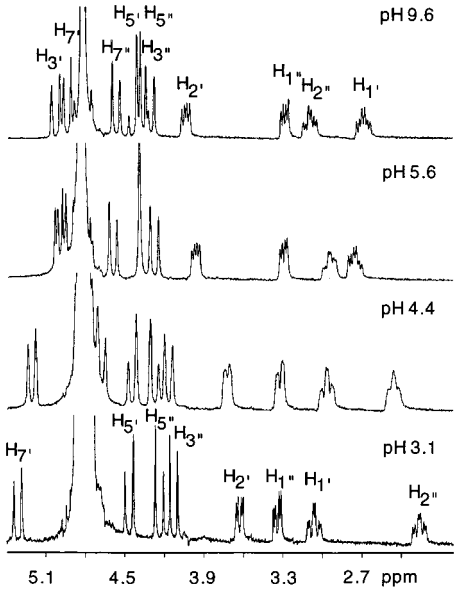

Figure 4. ^{1}H NMR spectra of $ReO(MEG_3H_2)$ (**10**) in D_2O at various pH values.

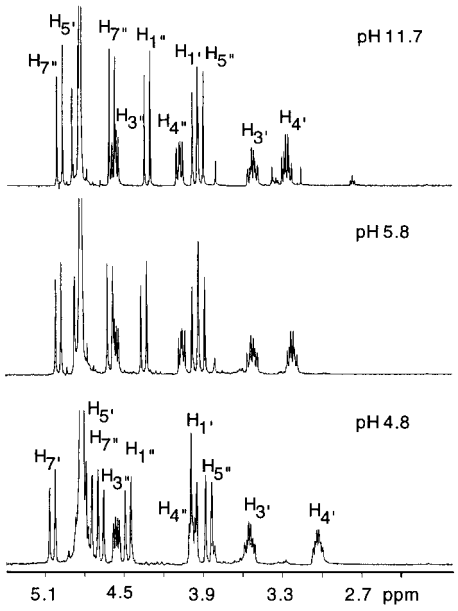

Figure 5. ^{1}H NMR spectra of $ReClO(MAEG_2H_3)$ (**11**) in D_2O from pH 11.7 to pH 4.8.

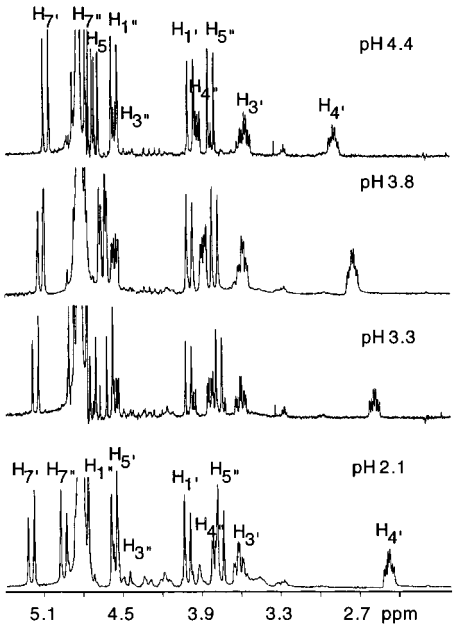

Figure 6. ^{1}H NMR spectra of $ReClO(MAEG_2H_3)$ (**11**) in D_2O from pH 4.4 to pH 2.1.

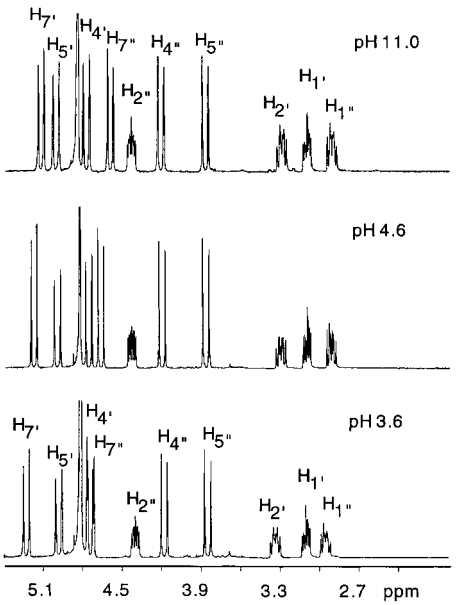

Figure 7. ^{1}H NMR spectra of $\{ReO(MECG_2H_2)\}_2$ (**12**) in D_2O at various pH values.

In summary, for all three complexes, the ^{1}H NMR spectra, monitored as a function of pH, exhibited changes only when the pH was below 6. This finding indicates that at physiological pH these complexes possess the desirable characteristic of existing as one isomeric species having only one ionization state, with the coordinated sp^3 N deprotonated. Thus, the N_3S ligands in all three complexes exhibit normal coordination at both physiological pH and pH ∼4.

Spectra of **10**−**12** were also obtained in DMSO-d_6. For **10**, the NH signal was a broad singlet at 9.20 ppm that disappeared immediately upon addition of D_2O, indicating rapid exchange of the NH proton. In comparison, the two NH signals (at 8.90 and 9.70 ppm) in the spectrum of **11** exhibited a much slower NH/D_2O exchange rate. (Five minutes after addition of a drop of D_2O, the intensity of the 8.9 ppm signal was approximately halved, while that of the 9.7 ppm signal was affected very little. Both signals had fully exchanged by the next day.) The downfield signal was assigned to the amide NH. No NH signals were observed in the DMSO-d_6 spectrum of **12**. For each complex, the COOH signal appeared as a broad singlet (12.34 ppm for **10**, 13.02 ppm for **11**, and 11.96 ppm for **12**).

Discussion

The strategy employed here to obtain new renal agents was to seek analogues with ligands intermediate between the EC-type and the MAG_3-type ligands but closer to the latter. Before discussing the results of these efforts, it is useful

Scheme 2

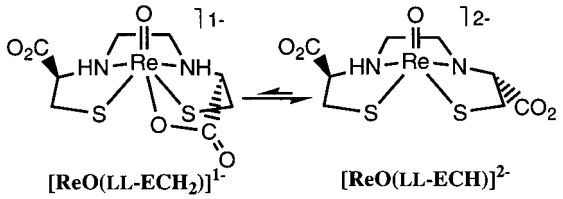

to understand some of the problems encountered in radiopharmaceutical design in general. A mixture of forms may adversely influence biodistribution of renal agents, as all components are unlikely to be cleared at the same rate or to have comparable protein binding affinities. An ideal renal agent should exist as a single isomer prepared without the need for chromatography and should have one ionization state at pH 7.4. However, mixtures of isomeric forms are frequently encountered in ^{99m}Tc(V)O radiopharmaceutical preparations.[13,14,29,30,43−45]

Most quadridentate ligands used in radiopharmaceutical preparations have directional character: that is, they are not C_2 symmetrcial when coordinated. All donors of the coordinated MAG_3 ligand in the widely used Tc-99m renal agent are either deprotonated amides or thiols, and the dangling carboxyl group is appended from one ligating sp^2 N donor. The acetyl bridging groups in the chelate ring favor a relatively planar geometry. Because the coordinated MAG_3 ligand has no asymmetric centers, the MO(MAG_3) (M = Re, Tc) complexes have only one geometric form; however, because the chelate ligand lacks C_2 symmetry, these complexes are chiral, with two enantiomers. The Tc-99m enantiomers have been separated and evaluated independently, showing small differences in plasma clearance and renal transit.[46,47] In contrast, the LL-ECH_6 ligand has C_2 symmetry and has the potential of forming a pure isomeric form of the Tc-99m renal agent. The enantiomer of the agent cannot be formed because no DD-ECH_6 is present in the preparation. However, we showed that ReO(LL-ECH_3) and the tetramethyl analogue, ReO(DD-$TMECH_3$) ($TMECH_6$ = ethylene-di-D-penicillamine, Chart 1), in solution exist as a mixture of monoanionic ligated CO_2^- and dianionic dangling deligated CO_2^- forms under physiological conditions (Scheme 2).[15] A secondary amine is protonated in the monoanion and is deprotonated in the dianion. Our evidence[15] is compelling that exactly this chemistry exists in the Tc-99m agent also.

The chirality of the M(V)O complexes can be viewed as arising from the different sense of disposition of the chelate around the M=O bond (clockwise vs counterclockwise).[48] If the ligand lacks C_2 symmetry and also has groups that project out of the equatorial plane when the ligand is coordinated, then the different sense of the disposition leads to syn and anti geometric isomers instead of enantiomers.[48] For example, if one replaces one glycyl group with an alanyl group in MAG_3, the mixture of enantiomers becomes a mixture of geometric isomers. In theory, conditions favoring one isomer could be found.

In pursuing the strategy of making the EC-type agents more like the MAG_3 agents, we had to circumvent these problems.[33,34,42] Specifically, we had to design agents which do not exhibit the persistent presence of both syn and anti isomers and which do not have ligands containing amines with pK_a values near physiological pH. We selected the monoamide−monoamine−dithiol (MAMA) class of chelates that typically form M(V)O(N_2S_2) (M = Tc, Re) complexes. Solid-state and solution studies of ReO($MAECH_2$) (L-$MAECH_5$ is mercaptoacetamide-ethylene-L-cysteine, cf. Chart 1) revealed that the syn and anti isomers both form.[34] At high pH, the syn isomer is thermodynamically preferred, and syn/anti equilibration forming 94% of the syn isomer was complete in an acceptable time (<30 min). Moreover, the pK_a of the monoanion of ReO(L-$MAECH_2$) is low (6.0); thus, the dianionic form of ReO($MAECH_2$) predominates at physiological pH. Evidence is strong that the Tc-99m analogue exists almost exclusively as *syn*-[^{99m}TcO(L-MAEC)]$^{2-}$, and the agent has excellent renal imaging properties in rats.[13,14] Thus, we are extending studies to human volunteers.

Because results obtained with MO(L-MAEC) (M = ^{99m}Tc, Re) were so promising, two isomers of the $MAECH_5$ ligand were prepared: cysteine−acetyl−cysteamine ($CACAH_5$) and cysteine−acetamide−ethanethiol ($CAATH_5$) (Chart 1). Chemical and biological studies of the ^{99m}Tc agents and Re complexes with these MAMA ligands demonstrated striking differences. Although *syn*- and *anti*-MO($CACAH_2$) isomers do not equilibrate at an observable rate,[33] the anti isomer of MO(D-$CAATH_2$) converted to the syn isomer upon heating. Thus, *syn*-ReO($CAATH_2$) has solution behavior similar to that of *syn*-ReO($MAECH_2$) but different from that of *syn*-ReO($CACAH_2$). The amine can adopt either an *endo*-NH or an *exo*-NH configuration. In the complexes of these MAMA ligands, the amine favors the *endo*-NH configuration even if the isomerization rates are different. Empirical evidence suggests that the *exo*-NH configuration should be unfavorable because the metal is usually displaced out of the basal plane toward an endo substituent.[40] From molecular mechanics calculations, structures with an *exo*-N(2)H are ∼6 kcal/mol less stable than the lowest-energy endo analogue.[42] A secondary amine donor of quadridentate ligands (e.g., EC-type ligands) prefers the endo configuration.[29,34,49]

The anti isomer of ^{99m}TcO(D-$CACAH_2$) has a higher rate of renal clearance than the syn isomer.[50] Preliminary bio-

(43) Canney, D. J.; Billings, J.; Francesconi, L. C.; Guo, Y.; Haggerty, B. S.; Rheingold, A. L.; Kung, H. F. *J. Med. Chem.* **1993**, *36*, 1032−1040.
(44) Kasina, S.; Fritzberg, A. R.; Johnson, D. L.; Eshima, D. *J. Med. Chem.* **1986**, *29*, 1933−1940.
(45) Vanbilloen, H. P.; Cleynhens, B. J.; Verbruggen, A. M. *Nucl. Med. Biol.* **2000**, *27*, 207−214.
(46) Verbruggen, A.; Bormans, G.; Cleynhens, B.; Hoogmartens, M.; Vandercruys, A.; De Roo, M. *Eur. J. Nucl. Med.* **1988**, *14*, 256 (abstract).
(47) Verbruggen, A.; Bormans, G.; Cleynhens, B.; Hoogmartens, M.; Vandercruys, A.; De Roo, M. *Nuklearmedizin* **1989**, *25*, 436−439.
(48) Hansen, L.; Marzilli, L. G.; Taylor, A. *Q. J. Nucl. Med.* **1998**, *42*, 280−293.
(49) Mahmood, A.; Baidoo, K. E.; Lever, S. Z. In *Technetium and Rhenium in Chemistry and Nuclear Medicine 3*; Nicolini, M., Bandoli, G., Mazzi, U., Eds.; Cortina International: Verona, 1990; pp 119−124.
(50) Hansen, L.; Xu, X.; Lipowska, M.; Taylor, A., Jr.; Marzilli, L. G. *J. Nucl. Med.* **1998**, *39*, 217P.

distribution studies[13] of ^{99m}TcO(CAATH$_2$) complexes in rats revealed selective and rapid renal excretion in urine for one isomer, *syn*-^{99m}TcO(D-CAATH$_2$). Although the Tc-99m agents formed from these MAMA ligands have desirable properties and deserve continued study in humans, they may not be sufficiently better than the clinically used agents to justify their widespread use. Consequently, the search for superior agents led us to pursue the second strategy and to investigate agents with ligand analogues of MAG$_3$H$_5$.

Like the MAMA ligands and MAG$_3$, the three MAG$_3$ ligand analogues have a directional character and lack C_2 symmetry. Compared to MAG$_3$, the three MAG$_3$ ligand analogues used in this study have one CO group replaced by a CH$_2$ group. Furthermore, we have varied the position of the CH$_2$ and CO groups. The resulting new ligands now have one ring that is puckered. Chemical[33,34,42] and computational[42] studies of the MAMA complexes all indicate that an *endo*-NH group is likely to be present in complexes of the MAG$_3$-like ligands. The solution NMR data and the solid-state structure for **10** confirm this similarity between MAMA and MAG$_3$-like complexes.

A consideration of the reasons for the unusual coordination mode of the MAEG$_2$H$_5$ ligand in complex **11** (Figure 2) provides valuable insight into ligand design. Normally, quadridentate ligands containing various combinations of thiol, amine, and amide donor groups form five-coordinate M(V)O complexes, with all four donor groups coordinated in the basal plane and the amide donor groups coordinated via the deprotonated nitrogen of the now negatively charged amido group. However, in **11**, the amide group of the terminal residue occupies the axial coordination site and binds through oxygen (O(3)) (Figure 2). Models reveal that this amide group is positioned near the axial coordination site by virtue of the conformation of the central chelate ring and the preferred[34] endo configuration of the ligated amine N(2). Also, the models suggest that the central chelate ring pucker is important. The central chelate ring adopts a pucker which places the C(4) methylene group endo to the oxo ligand (see Chart 2 for numbering). If the central chelate ring were to adopt the opposite pucker (with C(4) exo), the terminal amide group would be poised to coordinate in the equatorial position occupied by the chloro ligand in the structure. However, in this opposite pucker, the C(3) methylene group is endo to the oxo ligand. This position is unfavorable because chelate rings anchored by amido donors are nearly planar, and the plane of such rings normally slopes down and away from the oxo ligand.[33,34] This ring is also anchored by the S donor, and thus, coordination of the two good donors in the basal plane is an important stabilizing factor. The conformation of the central chelate ring found in the structure allows the C(3) (bound to the amido donor) to maintain an O(1)−Re−N(1)−C(3) torsion angle of $>90°$. Because C(4) is bound to a flexible amine donor, the acute O(1)−Re−N(2)−C(4) torsion angle (79.3°) is easily accommodated, thereby allowing coordination of the carbonyl oxygen.

Coordination by the amide oxygen is preferred over coordination by the amide nitrogen, because the latter would need to be deprotonated. The axial coordination site is opposite to the strong trans influence oxo ligand, however, and this site does not support amide deprotonation. Thus, the terminal amido group coordinates in the axial position via the carbonyl oxygen, driven in large part by the properties of the S-terminal chelate ring at the other end of the ligand. However, this novel compound would not have formed unless acid was present to favor formation of a neutral amide and a ligand (in this case, chloride) was present to occupy the now vacated equatorial site. This strong equatorial binding site is always occupied in M(V)O complexes (M = Re, Tc).

The complex formed by MECG$_2$H$_5$ converts under acidic conditions from a monomeric species to the dinuclear complex, **12** (Figure 3). In this case, the ligand occupying the strong equatorial site vacated on amide protonation is the carboxyl group of the other half of the dimer. Thus, the reasons why both **11** and **12** have very unusual coordination by the quadridentate ligands are very similar. Also, both complexes revert to normal monomeric ReO(N$_3$S) five-coordinate species when dissolved in solutions above pH 4; for both, the amide is deprotonated above this pH.

One consequence of the new ligand design is apparent in the monomeric form of **12**. The secondary amine anchors the two acetyl bridges. Thus, deprotonation of the NH group appears to be highly favored, and the secondary amine is a deprotonated N-donor at well below physiological pH. This acidic nature of the secondary amine is apparent in the NMR signals for **12** in DMSO-d_6. A clear signal for a CO$_2$H group establishes that **12** has become a monomer and also strongly suggests that the secondary amine has become deprotonated even in DMSO-d_6.

Conclusions

The new ligands designed here lead to compounds which do not exhibit the persistent presence of both syn and anti isomers and which do not have ligands containing amines with pK_a values near physiological pH. Although two complexes (**10** and **11**) have less acidic coordinated secondary amines than does **12**, the coordinated sp^3 N is fully deprotonated at physiological pH for the complexes of all three new ligands. The complexes exist in one form. Thus, we have achieved our goal of preparing a single isomer in one ionization form at physiological pH. Previous work with quadridentate ligands containing these donor groups within similar chelate rings produced Tc-99m agents with chemistry closely paralleling that found with Re at the macroscopic level. The new ligands are likely to form only one Tc-99m species under physiological conditions and are therefore candidates for biological testing in Tc-99m renal agents.

As discussed in the Introduction, the form isolated at the nonphysiological low pH (conditions normally needed to obtain solid complexes of adducts with dangling carboxyl groups) is not simply the derivative in the carboxylic acid form. Rather, in two examples here, we found that a rearrangement had occurred to form interesting, relatively rare compounds. This information reveals the breadth of

multidentate ligand coordination geometry and is of intrinsic chemical interest.

Acknowledgment. This work was supported by the National Institutes of Health (Grant DK38842). We thank Dr. Rene Lachicotte, then at the University of Rochester, for collecting some of the X-ray data. We also thank Dr. Kenneth Hardcastle of Emory University for useful discussions and for determining the structure of **12**, using instruments supported by NIH Grant S10-RR13673 and NSF Grant CHE 9974864 to the Emory X-ray Crystallography Center.

Supporting Information Available: Crystallographic data for **10**, **11**, and **12** including tables of positional parameters, bond distances and angles, anisotropic displacement coefficients, and H-atom coordinates. This material is available free of charge via the Internet at http://pubs.acs.org.

IC011325Z